Acta Geodyn. Geomater., Vol. 13, No. 4 (184), 409–418, 2016
DOI: 10.13168/AGG.2016.0023
journal homepage: https://www.irsm.cas.cz/acta

ORIGINAL PAPER

RADON RELEASE FROM UNDERGROUND STRATA TO THE SURFACE AND UNIAXIAL COMPRESSIVE TEST OF ROCK SAMPLES

Wei ZHANG [1,2,3,4]*, Dongsheng ZHANG [5], Lixin WU [3], Juanjuan LI [1] and Jixin CHENG [5]

[1] *IoT Perception Mine Research Center, National and Local Joint Engineering Laboratory of Internet Application Technology on Mine, China University of Mining & Technology, Xuzhou 221008, P. R. China*
[2] *State and Local Joint Engineering Laboratory for Gas Drainage & Ground Control of Deep Mines, Henan Polytechnic University, Jiaozuo 454000, P. R. China*
[3] *School of Environment Science and Spatial Informatics, China University of Mining & Technology, Xuzhou 221116, P. R. China*
[4] *Key Laboratory of Safety and High-efficiency Coal Mining, Ministry of Education, Anhui University of Science & Technology, Huainan, 232001, P. R. China*
[5] *School of Mines, China University of Mining & Technology, Xuzhou 221116, P. R. China*

**Corresponding author's e-mail:* zhangwei@cumt.edu.cn

ARTICLE INFO

Article history:
Received 7 November 2015
Accepted 29 June 2016
Available online 13 July 2016

Keywords:
Underground strata
Radon release
α measurement
Uniaxial compressive test
Degree of correlation

ABSTRACT

The mechanism and critical conditions of rock failure in underground coal mining processes have attracted great attention. Based on the origin and properties of radon gas, we propose that radon release from underground strata to the surface occurs in two stages, i.e., the formation of free radon and the migration of radon gas. Due to its optimal combination of efficiency and low background measurements, the α-ray measurement was employed to measure radon gas from rock fracturing. The uniaxial compression of rock samples and the concentrations of radon emanating from the loaded samples were experimentally investigated. The results revealed that radon concentrations are negatively related to uniaxial loads and elastic deformations, provided compressive failures are not observed. As the loads increase, the stabilization duration and internal porosity of rock samples get decrease, which result in reduced radon emanation. When the load gets more than the limit strength of rock samples, the radon concentrations increase significantly and eventually reach the maximum value, and then slightly decrease and approximately tend to be stable. Finally, a preliminary correlation between the complete stress-strain process of uniaxial loaded rock samples and the concentration of radon emanated was presented, which needs further experimental validations. Even so, we believe that the failure mechanisms of mining-induced overburdens could be investigated based on radon gas concentrations.

1. INTRODUCTION

Since its discovery by Dorn in 1900, radon (^{222}Rn) and its decay products have attracted increasing attention globally. Generated continuously from radium (^{226}Ra) within the underground strata as an intermediate decay product of the uranium (^{238}U) radio-active series, which is present in terrestrial materials like rocks, soil, coal beds, and water, radon is a radioactive inert gas existing in the natural environment. Radon can be detected at low concentrations due to its radioactivity, and it accumulates in micro-cracks and pores due to its inert nature. Due to its unique physical and chemical properties, radon gas has been deployed to provide solutions to various problems. As a result, radon measurement has been intensively studied and applied in the following contexts:

1. Pollution controls and healthcare. (a) Prevention of indoor pollution. Radon is a colorless and odorless radioactive gas that can cause severe damage to human body (Lamonaca et al., 2014), including an increased probability of lung cancers, when it is present in concentrations above 200 Bq/m^3. (b) Healthcare. The presence of radon at low concentrations promotes sterilization, making it useful in healthcare (Al-Zoughool and Krewski, 2009).
2. Geological engineering. (a) Exploration of underground mineral resources. Radon could provides a valuable reference for the exploration of uranium resources. Based on soil radon measurement, solid state nuclear tracking, and trace element analysis, Roy et al. (2004) predicted the distribution of U-bearing breccia mineral deposit in Kuchanapalle, India. (b) Exploration of geothermal energy and bedrock underground water. Jalili-Majareshin et al. (2012) depicted the distribution of prospective areas of geothermal energy in Sarein, Iran, based on radon measurement. (c) Detection of buried structures such as faults. Walia et al. (2010) reported that N_2 is the most probable carrier gas of He, whereas CO_2 seems to be a good carrier gas of Rn in the vicinity of the Hsinhua fault zone. The trace of Hsinhua fault and neotectonic features can be identified from the spatial distribution of studied gases with a clear anomalous trend ENE-SWS. (d) Prediction of geological disasters such as

Cite this article as: Zhang W, Zhang D, Wu L, Li J, Cheng J: Radon release from underground strata to the surface and uniaxial compressive test of rock samples. Acta Geodyn. Geomater., 13, No. 4 (184), 409–418, 2016. DOI: 10.13168/AGG.2016.0023

earthquakes and volcanic eruptions. Cigolini et al. (2007) investigated earthquake-volcano interactions by using a network for radon monitoring at Stromboli volcano, which suggests a possible link between magma chamber volume, gaseous transfer and dynamic response of the volcano to near field seismic triggering.

3. Improvement in mines for safety. (a) Locating spontaneous combustion regions. Previous studies revealed that spontaneous combustion sites could be located rapidly by monitoring radon concentrations in the atmosphere (Zhao and Wu, 2003; Xue et al., 2008). (b) Locating hidden mined-out areas. Gao et al. (2012) used radon detection to estimate the scope of the goaf area. Herein, comprehensive geophysical methods (CGM) were successfully used to estimate the grouting quality of the goaf area under the surface railway, including vertical electrical sounding (VES), electromagnetic wave (EW) and seismic wave (SW). (c) Coal and gas outburst prediction. Wysocka (2010) started observations of changes of radon concentration in gas, sampled from headings, driven in endangered coal seams. Then, he reported that there is a degree of correlation between the temporal and spatial variations of radon level and the hazard level of an outburst, and it is possible to develop a "radon outburst's indicator" to support other methods of prediction of very dangerous geodynamic phenomena.

In spite of significant advancements, radon measurement techniques have not been widely applied in areas other than pollution controls, healthcare, geological engineering, and mining safety. Previously, we proposed a qualitative approach for ground detection of mining-induced overburden fissures using radon measurement (Zhang et al., 2011, 2014). Due to severe problems caused by rock mass failures in the underground coal mining process, the mechanism and critical conditions of rock mass failure have attracted attention from the field of rock mechanics, where specialists have employed techniques including microseismics, acoustic emission, electromagnetic radiation, electrical approaches, and ultrasonic waves to study the issues (Frid and Vozoff, 2005; Triantis et al., 2008; Chaki et al., 2008; He et al., 2010; Amitrano et al., 2010). Although much studies have dealt with radon emission from rocks under axial loading, mainly focusing on granite, tuff, lava, marble, crystalline rock, concrete and so on (Holub and Brady, 1981; King and Luo, 1990; Tuccimei et al., 2010; Mollo et al., 2011; Nicolas et al., 2014; Koike et al., 2015), very few literatures have studied the correlation between radon concentrations and rock deformations (especially rock samples from the coal-bearing strata), which is the key for advance prediction of mining-induced fractures evolution and overburden failure in mining engineering. This paper investigates the release process of underground radon based on the generation and properties of radon; it also determines the object of radon measurement. Additionally, uniaxial compression of rock samples and concentrations of radon emanated in this process were experimentally investigated, which will provide a theoretical basis for radon detection of mining-induced fractures in the overlying strata.

2. THE FORMATION AND PROPERTIES OF RADON

2.1. FORMATION OF RADON

Radon is a direct decay product of radium. The three natural isotopes of radon are ^{219}Rn, ^{220}Rn and ^{222}Rn, with half-lives of 3.96 s, 55.6 s and 3.82 d, respectively. Due to the extremely low concentration of ^{219}Rn in the crust and its short half-life (Baixeras et al., 2001), this isotope is usually undetectable. Similarly, only a small amount of ^{220}Rn is released from the crust, and it decays quickly due to its short half-life. Indeed, the concentration of ^{220}Rn in the crust is only 10 % that of ^{222}Rn, and the overall quantity of natural ^{222}Rn is significantly larger than that of natural ^{219}Rn and ^{220}Rn. Additionally, the half-life of ^{222}Rn is much longer than that of the other two isotopes. Therefore, the term "radon" refers to ^{222}Rn in most cases, including this study.

2.2. PROPERTIES OF RADON

2.2.1. PHYSICAL PROPERTIES

Radon is gaseous in its uncombined form, and it is a natural radioactive, colorless, odorless, and tasteless inert gas. Under standard pressures, gaseous radon converts to a liquid at -65 °C, which then converts to a solid at -113 °C. The melting and boiling points of radon are -71 °C and -61.8 °C, respectively. The density of radon is 9.73 kg/m^3, which is 7.5 times the air density.

In geological environments, radon exhibits significant capability to migrate into the atmosphere. Furthermore, radon is highly soluble in water and organic solvents like toluene, petroleum and ethanol; its solubility and inertness allow it to migrate with underground water. The solubility of radon decreases as the temperature increases (Schubert et al., 2012), and its dissolution rate declines once its concentration in the solvent exceeds the saturation point.

2.2.2. CHEMICAL PROPERTIES

Radon is an inert element with an atomic number of 86. Radon isotope atoms are electrically neutral with an atomic radius of 1.2×10^{-10} m, and molecules are monatomic. Its electron distribution is $6s^26p^6$ (Figure 1), indicating that the outer layer holds eight electrons. Hence, radon is a typical atmophile element and exists naturally in gaseous form.

With a decay constant of 2.097×10^{-6}/s, it takes 30 d for the decay of radium into radon to reach radioactive equilibrium. The energy and range in the atmosphere of α particles generated in the decay of radon are 5.481 MeV and 4.04 cm, respectively. Although it is an inert gas, radon can be readily

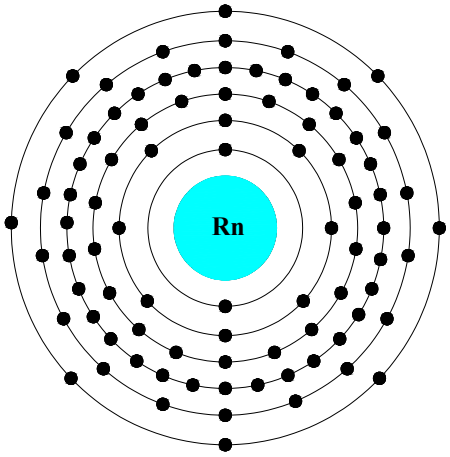

Fig. 1 Electron distribution of radon nucleus.

absorbed by solid materials such as activated carbon, rubber, paraffin, SiO_2, and Al_2O_3 (Rama and Moore, 1984), of which activated carbon shows the best adsorption capability.

3. RADON RELEASE FROM UNDERGROUND STRATA TO THE SURFACE

Radon is generated in environments such as underground rocks, coal beds, and soils, after which it migrates up to the surface and escapes to the atmosphere. This whole process can be called as radon release. The radon release process can be divided into two stages: the formation of free-state radon and the migration of radon gas. In the first stage, radium atoms in underground strata decay by emitting alpha particles, which generate radon atoms. The nuclear recoil effect and emanation effect lead the generated radon atoms to diffuse from the rock lattice to connected micro-cracks and become free-state radon. In the second stage, free-state radon migrates to the surface via cracks and pores and escapes to the atmosphere. Figure 2 shows the radon release process.

3.1. FORMATION OF FREE-STATE RADON

Radon atoms formed in the α-decay of radium atoms have a recoil kinetic energy of 8.6×10^4 eV according to the energy conservation principle, resulting in a considerable recoil distance from the parent atom. This is referred to as the nuclear recoil effect. The composition and density of the decay medium determine the recoil distance of radon atoms (Nguyen et al., 2005). For instance, recoil distances of radon atoms in solid matters and water are 20-70 nm and 100 nm, respectively. Nevertheless, not all radon atoms resulting from radium decay migrate. After the recoil motion, some atoms remain stuck in the original lattice or enter another lattice. In these cases, radon atoms are not able to escape as the brown motion does not generate sufficient kinetic energy, and these atoms make no contribution to radon emanation. Hence, this study focuses on free-state radon.

The radon emanation effect can be defined as escape of a radon atom from a Ra-bearing grain into pore spaces (Sakoda et al., 2011). The nuclear recoil effect plays a key role in radon emanation. The ratio of free-state radon generated by the nuclear recoil

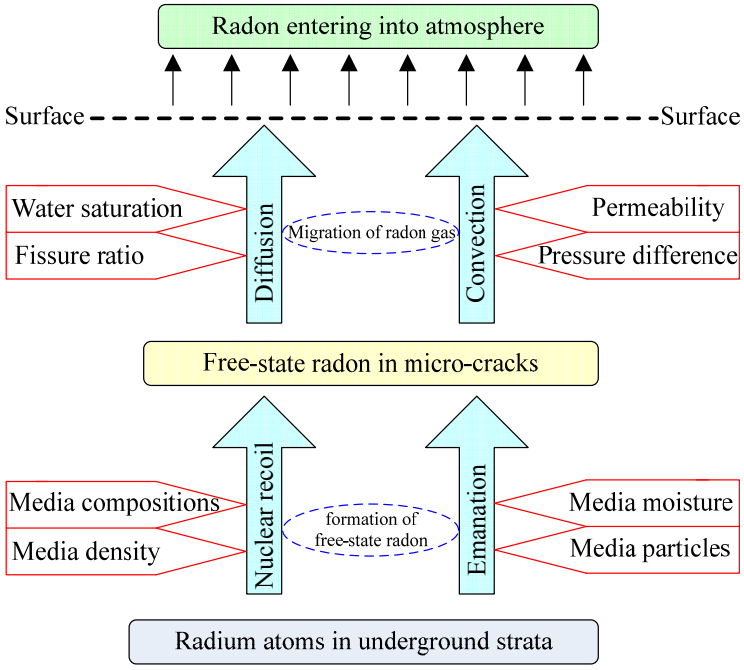

Fig. 2 Radon release from underground strata to the surface.

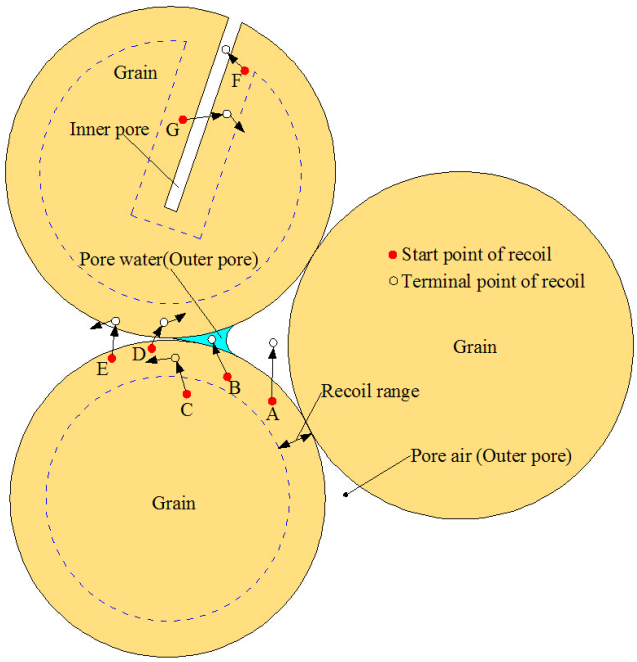

Fig. 3 Sketch of radon emanation effect.

effect to overall radon content in the rock medium can be defined as the emanation coefficient (Ferry et al., 2002). The emanation coefficient determines the quantity of free-state radon in the rock formation. It is related to the moisture content of the medium and the fragment particle diameter. Figure 3 shows the phenomenon of radon emanation effect. Radon in points (A, B, E and F) is regarded as being emanated, while points (C, D and G) are not emanation. If radon cannot diffuse out from the inner pore into outer, radon in point (F) should not be regarded as being emanated. Arrows following terminal points of recoil represent diffusion process, which is not to scale.

3.2. MIGRATION OF FREE-STATE RADON

This section discusses the upward migration of radon gas from underground strata. Due to its unique physical and chemical properties, radon gas migration is related to various factors, and no agreement has been reached on the mechanism and principles underlying this process. Various studies have proposed different mechanisms of radon gas migration from underground strata to the surface (e.g., Wilkening and Watkins, 1976; Fleischer and Mogro-Campero, 1979; Soonawala and Telford, 1980; Varhegyi et al., 1992; Folger et al., 1997; Wattananikorn et al., 1998; Cameron et al., 2002; Le and Wang, 2006), including diffusion, convection, pore fluid, advection, and micro-bubbles as carriers, relay transmission, stress compression, and cluster theory. Nevertheless, different groups have uniformly reported that radon gas can migrate to the ground via micro-cracks and pores in the underground strata. Furthermore, diffusion and convection effects are two mechanisms that have been widely accepted to explain the radon migration process. (a) Diffusion effect. Proposed in the 1930s, the diffusion mechanism of radon migration remains a major theory for this phenomenon (Nazaroff, 1992). Generally, the diffusion coefficient describes the migration capability of radon gas in a certain medium, as determined by water saturation and fissure ratio. The diffusion of radon gas can be described by Fick's First Law. (b) Convection effect. The convection effect is the second dominant mechanism commonly accepted for radon gas migration (Malmqvist et al., 1989). Generally, the convection flow rate describes the migration capability of radon gas in a certain medium, as determined by medium permeability and pressure difference. The convection of radon gas can be described by Darcy's Law.

4. DETERMINATION OF MEASUREMENT OBJECTS FOR RADON GAS

In the radioactive decay process of ^{238}U series, ^{214}Pb and ^{214}Bi, as the decay products of ^{222}Rn, are the major irradiators of gamma rays (γ-rays), accounting for 98 % of radiation. Hence, these daughter nuclides were taken as the measuring objects for γ-ray. Similarly, ^{218}Po, a first generation decay product with a short half-life (3.1 minutes), was taken as the measuring object for alpha rays (α-rays). To date, various approaches based on the same principles have been reported for radon measurement, although sampling process and measuring sites have varied (Winkler et al., 2001; Gutierrez, et al., 2004). This study measured radon based on α-ray measurement, as the weak penetration capability of α-ray enables low environmental background measurement, resulting in high detection sensitivity. Besides this, α detectors

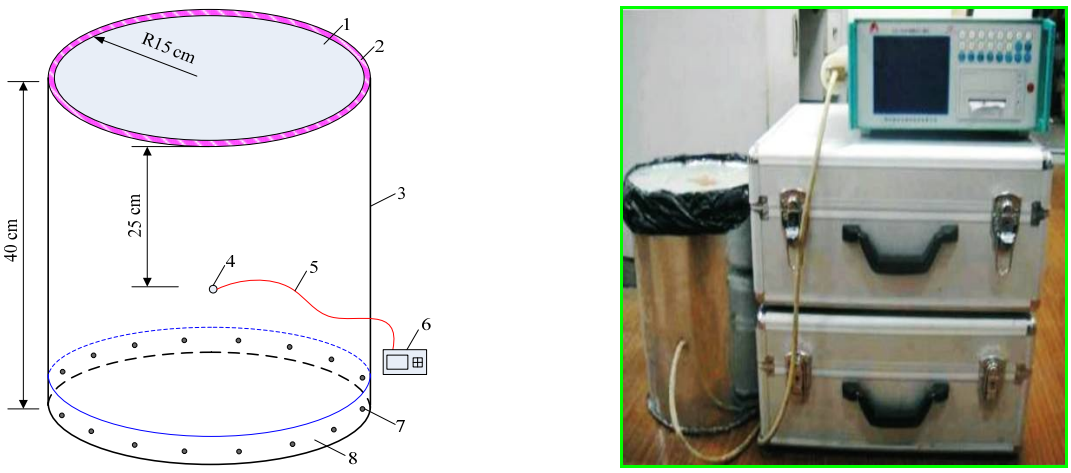

a) b)

Fig. 4 SRRS: (**a**) schematic illustration; (**b**) physical set-up. 1, movable cover; 2, sealing gasket; 3, container wall; 4, connecting hole; 5, rubber hose; 6, CRD; 7, rivet; 8, container bottom.

exhibit excellent efficiency, thus further improve the accuracy of α-ray measurement. Based on the above analysis, the continuous radon detector (CRD) (KJD-2000R, Xstar Company, China) has been chosen as the radon measuring instrument. The CRD has greater sensitivity than is 1.3 cpm/(Bq/m^3) with measurement range 2 to 400,000 Bq/m^3. Prior to use of the CRD ex works, it was calibrated in the standard radon chamber (SRC) of China's National Institute of Metrology (CNIM). The calibration process includes three steps: (1) A stable radon concentration will be produced in the SRC; (2) The benchmark instrument (Alpha-GUARD PQ2000 emanometer, Genitron Company, Germany) will be used; (3) A comparative measurement will be conducted, and the scale factor of the device will be calibrated. To guarantee the measurement accuracy of the CRD, it will be sent periodically to the CNIM for inspection every six months.

5. UNIAXIAL COMPRESSIVE TESTS OF ROCK SAMPLES

Radon emanation in rocks under uniaxial compression was investigated using a self-designed radon release set-up (SRRS) and an electro-hydraulic servo-controlled rock mechanics testing system (MTS Model 815, MTS Company, America) at the State Key Laboratory of Coal Resources and Safe Mining (SKLCRSM), Xuzhou, China.

5.1. DESIGN OF SRRS

Figure 4 illustrates the SRRS used in this study, which consists of a CRD, container, rubber hose, and sealing gasket.

Characteristics of SRRS are as follows:

1. The container is made of a stainless steel cylinder with a diameter of 30 cm and a height of 40 cm. It has a movable cover, rivet-fixed bottom, and a connecting hole with a diameter of 5 mm at a point 25 cm from the top of the wall.
2. The CRD is connected to the container by a rubber hose with a diameter of 5 mm. More specifically, the connecting hole on the container wall is connected to the CRD's inlet.
3. In order to improve container sealing and therefore measurement accuracy, a sealing gasket is included between the movable cover and the wall. Meanwhile, the joints between the bottom and the wall are sealed using glassy cement, and the connecting hole is covered by butter and sealed by plastic film.

5.2. SAMPLE MACHINING AND LOADING EQUIPMENT

Originating from the #6203 coalface of Baoshan Coal Mine in Shenfu-Dongsheng Coalfield, the rock samples used were obtained by a combination of ground drilling and underground sampling. The samples were 0.3~0.65 mm particles of pelitic siltstones consisting of feldspar, quartz and Ca/Fe gel. According to relevant standards (Fairhurst and Hudson, 1999), samples were cored into cylinders (#1~#4) with diameters and heights of 50 mm and 100 mm, respectively. Then, the cylinders were polished so that the difference in parallelism of the two end surfaces was less than 0.02 mm, the perpendicularity of the two end surfaces to the sample axis was less than 3.5'', and the surface roughness of the cylinder side-wall was less than 0.3 mm. Finally, polished samples were dried for 24 hours, and they were sealed before being used for the uniaxial compressive tests. The uniaxial compressive tests were conducted using a rigidity servo testing system with a maximum axial pressure of 4600 kN and a loading rate in the rage of 0.1~0.5 kN/s. Loading and strains were measured using a dynamic strain meter.

a) b) c)

Fig. 5 Experimental procedures for radon gas emanation measured: (**a**) before compression; (**b**) during compression; (**c**) after compression.

5.3. EXPERIMENTAL PROCEDURES

First, the sealing of the experimental setup was checked before allowing 1 min pre-functioning of the radon detector. Samples #1~#4 were placed in the container, and concentrations of radon gas emanating at different points before compression, during compression, and after compression were measured every 5 min. Figure 5 shows the experimental procedures.

5.4. EXPERIMENTAL RESULTS

5.4.1. RADON CONCENTRATIONS AND AXIAL DEFORMATIONS VERSUS LOADING TIME UNDER DIFFERENT UNIAXIAL LOADS (SAMPLES #1~#3)

Uniaxial compressive test results show that as the uniaxial load reached to above 75.2 kN, the samples (#1~#3) got cracked and eventually failed. Therefore, the uniaxial loads used in this section study were 20 kN, 40 kN, and 60 kN. When a constant load (10 kN) was given to the samples #1~#3 after 5 min, radon concentration measurement was conducted. Figure 6 charts the radon concentrations and axial deformations of sample #1~#3 against loading time under different uniaxial loads. Uniaxial deformations of these samples increased and eventually saturated before samples failure. This process can be divided into three stages, including transient loading strain, attenuated strain, and allostasis. Although we no have microphotographs of rock microstructures, acoustic emissions or porosity data, based on the variation features of radon concentrations, an inference can be made as follows: Initially, uniaxial deformations and strain rates of the samples were relatively high, indicating compression of the internal open structures and micro-cracks. As the loading time increased, the rate of axial deformations decreased. The results also revealed that uniaxial deformations were positively related to uniaxial loads, and the loading time for deformations to reach the saturation level and samples internal porosity decreased as the uniaxial loads increased.

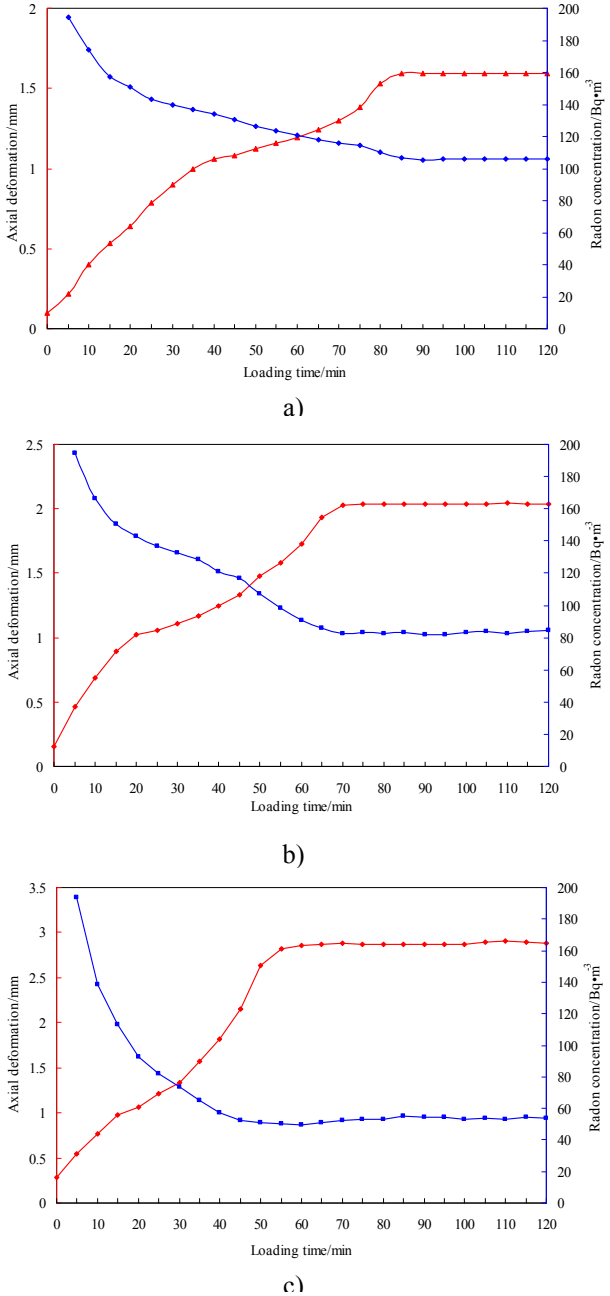

Fig. 6 Radon concentrations and axial deformations versus loading time under different uniaxial loads: (**a**) 20 kN; (**b**) 40 kN; (**c**) 60 kN.

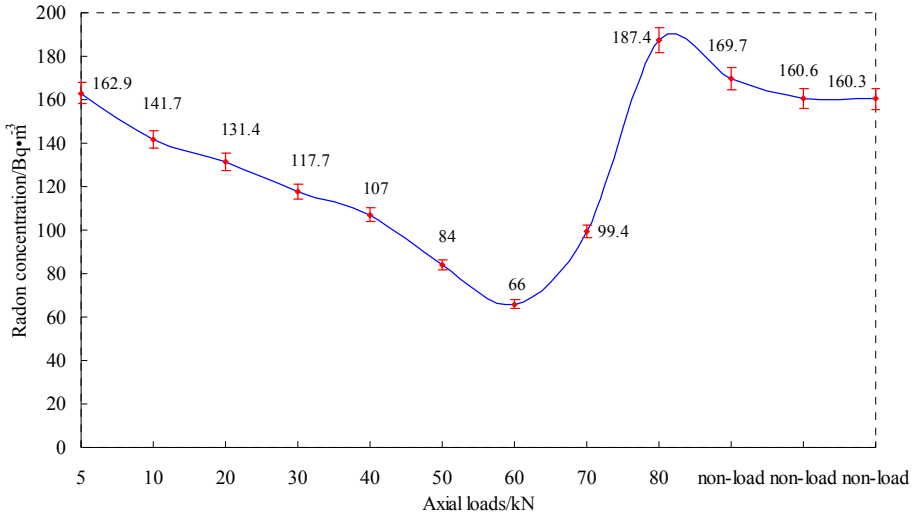

Fig. 7 Concentrations of radon gas emanated under different uniaxial loads.

5.4.2. CONCENTRATIONS OF EMANATED RADON GAS UNDER DIFFERENT UNIAXIAL LOADS (SAMPLE #4)

Uniaxial compressive test results show that as the uniaxial load reached to above 75.6 kN, the sample #4 got cracked and eventually failed. Therefore, the uniaxial loads used in this section study were 10 kN, 20 kN, 30 kN, 40 kN, 50 kN, 60 kN, 70 kN and 80 kN. When a constant load (5 kN) was given to the sample #4 after 5 min, radon concentration measurement was conducted. In this test, every load will be proceeded for 2 hours. When the sample was uniaxially loaded up to failure, the radon measurement also would be operated for 6 hours. Figure 7 charts the radon concentrations of sample #4 under different uniaxial loads. It is well-known that radioactive materials are composed of large radioactive atoms, whose radioactive decay has the features as contingency and randomness. Therefore, a statistical fluctuation phenomenon of radioactive decay frequently appears in the process of actual measurement, which causes a statistical fluctuation error and becomes the main source of experimental errors (Winkler et al., 2001). Under laboratory conditions, environmental factors (which mainly include temperature, humidity and pressure) can be easily kept in a constant state. In order to decrease the degree of influence on the experimental results from the natural fluctuation errors, the accumulating average values of measured data (whose statistical fluctuation errors were within 4%) had been adopted. Therefore, it is thought that the degree of statistical fluctuation is small, and the experimental errors will not significantly affect the subsequent results analysis. According to Figure 7, we can draw a conclusion as follows: when the loads within 60 kN, concentrations of radon gas emanated decreased slowly as the uniaxial loads increased, indicating that uniaxial compression gradually compacted the migration channels for radon gas, and the new exhaling surfaces do not form. A negative correlation between radon emanation amount and uniaxial loads is presented. When the load is above 60 kN, the radon concentrations increased significantly and eventually reached the maximum value, which indicated that the new large micro-cracks had further propagated and the sample had failed finally. Moreover, radon concentrations slightly decreased and approximately tended to be stable.

6. DISCUSSION

6.1. THE PRELIMINARY CORRELATION BETWEEN COMPLETE STRESS-STRAIN CURVES AND RADON EMANATION

Based on the uniaxial compressive tests results, we could audaciously draw a theoretical hypothesis as the following schematic cartoon. Figure 8 shows a preliminary correlation between complete stress-strain curves and radon emanation. Five stages maybe were found. At the first stage (Section *OA*, compacting of micro-cracks), the uniaxial strain was large, and the compressive pressure closed internal pores, resulting in decreased radon concentrations (Section *O'A'*). At the second stage (Section *AB*, elastic deformation), the stress-strain curves were linear and no cracks were initiated, resulting in stabilized radon concentrations (Section *A'B'*). At the third stage (Section *BC*, crack initiation), new internal cracks were initiated, and large cracks were observed as the axial stress increased. As a result, the concentrations of radon increased significantly (Section *B'C'*). At the fourth stage (Section *CD*, steady crack propagation), propagation and growth of cracks corresponded with increased axial stress, resulting in considerable vibrations and increased internal crack surfaces. As a result, radon concentrations increased significantly (Section *C'D'*). At the fifth stage (Section *DE*, crack propagation and sample failure), micro-cracks aggregated as the loading increased; cracks were observed until sample failure. At this stage, concentrations of radon maximized and stabilized (Section *D'E'*). The above preliminary correlation is only an inference, which needs more experimental validations (including coal and rock samples tests, uniaxial and triaxial experiments) in further studies.

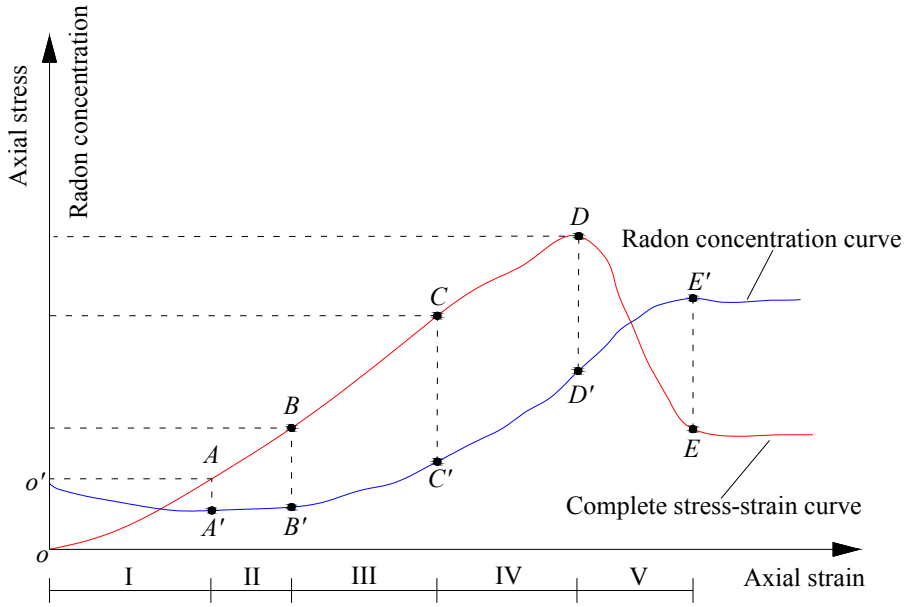

Fig. 8 Schematic cartoon of correlation between overall stress-strain curves and radon emanation.

6.2. REQUIREMENTS FOR FUTURE RESEARCH

The radon concentration in underground strata is influenced by a number of factors. These may include the concentrations of uranium and thorium in the strata, the radon emanation power of the materials, the physical properties of the materials (e.g., the diffusion coefficient, the mineral particle size, the permeability, and the porosity) and the environmental factors (e.g., the moisture content, the surrounding stress, atmospheric pressure, Earth tides, and the temperature) (Sun and Furbish, 1995; Hutter, 1996; Garver and Baskaran, 2004; Cigolini et al., 2009; Xue et al., 2010; Perrier and Girault, 2013). However, the degree of influence of these factors varies with the different types of rock, coal, soil, and strata. The experimental results reported in this paper are based on limited rock samples with a specific condition. Therefore, more additional studies are necessary such as the following:

(a) A series of laboratory tests are necessary in order to investigate the effect of uncertain factors, such as strata types, moisture content, mineral particle size, and radon concentration in strata, especially reduce the degree of influence due to the environmental factors that can affect the radon variability. This is the most elementary study for radon detection technique in mining engineering.

(b) If the experimental conditions are allowable, the multi-parameter information should be synthetically considered. In recent years, some studies have investigated the detection of other forms of energy (e.g., acoustic emission, electromagnetic emission and neutron emission) as a new method for the monitoring of rock fracturing phenomena. Therefore, we should consider using the detection of other forms of energy together with radon measurement for our research.

7. CONCLUSIONS

1. As described in the introduction, we have used radon measurement to detect the evolution process of mining-induced fractures in overburden. Although those studies are based on specific detection conditions and limited measured data, the results suggest that the radon detection of mining-induced fractures from overlying strata to the surface is feasible. Now, we need to understand the quantitative correlation between radon concentrations and rock deformations for advance prediction of mining-induced fractures evolution and overburden failure, which is expected to reduce the development of the mining-induced fractures for the mitigation of safety issues as well as the adverse environmental consequences, this is also the eventually aim of this study.
2. Radon emanation can be divided into two stages, i.e., the formation of free-state radon and the migration of radon gas. Through the nuclear recoil effect and emanation effect, radon atoms generated from radium diffuse from rocks to micro-cracks and become free-state radon. In the second stage, free-state radon migrates to the ground via cracks and pores by diffusion and convection mechanisms, eventually escaping into the atmosphere.
3. Before rock samples failure, the elastic deformations were positively and radon concentrations were negatively correlated with the uniaxial loads. Furthermore, the time for deformations to reach the saturation level and internal porosity of samples decreased as the uniaxial loads increased, resulting in decreased radon emanation. When the load got more than the limit strength of rock samples, the radon concentrations increased significantly and eventually reached the maximum value as samples failure, and finally tended to be stable.

4. The presented preliminary correlation is only an inference that needs more experimental validations in further studies, such as coal and rock samples tests, uniaxial and triaxial experiments and multi-parameter information consideration. Even so, we believe that the failure mechanisms of mining-induced overburdens could be investigated based on radon gas concentrations.

ACKNOWLEDGMENTS

The research is financially supported by the National Basic Research Program of China (No. 2015CB251600), the National Natural Science Foundation of China (No. 51404254), the China Postdoctoral Science Foundation (Nos. 2014M560465 and 2015T80604), the Jiangsu Planned Projects for Postdoctoral Research Funds (No. 1302050B), the Research Fund of State and Local Joint Engineering Laboratory for Gas Drainage & Ground Control of Deep Mines (No. G201604) and the Research Fund of Key Laboratory of Safety and High-efficiency Coal Mining, Ministry of Education (No. JYBSYS2015106). We wish to thank the Baoshan Coal Mine for supporting the important work, as well as Xiaofu Zhang from Inner Mongolia Yitai Coal Limited for the assistance of rock samples collection. Special thanks are given to doctors Mengtang Xu from the Guizhou Institute of Technology for his experimental assistance, and Chengguo Zhang from the University of New South Wales, for his language assistance. The authors are also grateful to the editor and anonymous reviewers for their constructive comments and helpful recommendation.

REFERENCES

Al-Zoughool, M. and Krewski, D.: 2009, Health effects of radon: A review of the literature. International Journal of Radiation Biology, 85, No. 1, 57–69. DOI: 10.1080/09553000802635054

Amitrano, D., Arattano, M., Chiarle, M., Mortara, G., Occhiena, C., Pirulli, M. and Scavia, C.: 2010, Microseismic activity analysis for the study of the rupture mechanisms in unstable rock masses. Natural Hazards and Earth System Sciences, 10, No. 4, 831–841. DOI: 10.5194/nhess-10-831-2010

Baixeras, C., Erlandsson, B., Font, L. and Jonsson, G.: 2001, Radon emanation from soil samples. Radiation Measurements, 34, No. 1-6, 441–443. DOI: 10.1016/S1350-4487(01)00203-7

Cameron, E.M., Leybourne, M.I. and Kelley, D.L.: 2002, Exploring for deeply covered mineral deposits: formation of geochemical anomalies in northern Chile by earthquake-induced surface flooding of mineralized groundwaters. Geology, 30, No. 11, 1007–1010. DOI: 10.1130/0091-7613(2002)0302.0.CO;2

Chaki, S., Takarli, M. and Agbodjan, W.P.: 2008, Influence of thermal damage on physical properties of a granite rock: porosity, permeability and ultrasonic wave evolutions. Construction and Building Materials, 22, No. 7, 1456–1461. DOI: 10.1016/j.conbuildmat.2007.04.002

Cigolini, C., Laiolo, M. and Coppola, D. 2007, Earthquake–volcano interactions detected from radon degassing at Stromboli (Italy). Earth and Planetary Science Letters, 257, No. 3, 511–525. DOI: 10.1016/j.epsl.2007.03.022

Cigolini, C., Poggi, P., Ripepe, M., Laiolo, M., Ciamberlini, C., Delle Donne, D., Ulivieri, G., Coppola, D., Lacanna, G., Marchetti, E., Piscopo, D. and Genco, R.: 2009, Radon surveys and real-time monitoring at Stromboli volcano: influence of soil temperature, atmospheric pressure and tidal forces on 222Rn degassing. Journal of Volcanology and Geothermal Research, 184, No. 3-4, 381–388. DOI: 10.1016/j.jvolgeores.2009.04.019

Fairhurst, C.E. and Hudson, J.A.: 1999, Draft ISRM suggested method for the complete stress-strain curve for intact rock in uniaxial compression. International Journal of Rock Mechanics and Mining Sciences, 36, No. 3, 279–289. DOI: 10.1016/S0148-9062(99)00006-6

Ferry, C., Richon, P., Beneito, A., Cabrera, J. and Sabroux, J.C.: 2002, An experimental method for measuring the radon-222 emanation factor in rocks. Radiation Measurements, 35, No. 6, 579–583. DOI: 10.1016/S1350-4487(02)00092-6

Fleischer, R.L. and Mogro-Campero, A.: 1979, Radon enhancements in the Earth: evidence for intermittent upflows?. Geophysical Research Letters, 6, No. 5, 361–364. DOI: 10.1029/GL006i005p00361

Folger, P.F., Poeter, E., Wantye, R.B., Day, W. and Frishman, D.: 1997, ^{222}Rn transport in a fractured crystalline rock aquifer: results from numerical simulations. Journal of Hydrology, 195, No. 1-4, 45–77. DOI: 10.1016/S0022-1694(96)03243-X

Frid, V. and Vozoff, K.: 2005, Electromagnetic radiation induced by mining rock failure. International Journal of Coal Geology, 64, No. 1, 57-65. DOI: 10.1016/j.coal.2005.03.005

Gao X., Zhang X., Wang X., Song, D.G., Hu, X.W., Peng, Y.L., Zheng, Y.X. and He, X.: 2012, Study on comprehensive geophysical prospecting methods on detection of complex goaves grouting quality. Journal of Convergence Information Technology, 7, No. 23, 308–316.

Garver, E. and Baskaran, M.: 2004, Effects of heating on the emanation rates of radon-222 from a suite of natural minerals. Applied Radiation and Isotopes, 61, No. 6, 1477–1485. DOI: 10.1016/j.apradiso.2004.03.107

Gutierrez, J.L., Garcia-Talavera, M., Pena, V., Nalda, J.C., Voytchev, M. and Lopez, R.: 2004, Radon emanation measurements using silicon photodiode detectors. Applied Radiation and Isotopes, 60, No. 2-4, 583–587. DOI: 10.1016/j.apradiso.2003.11.080

He, M.C., Miao, J.L. and Feng, J.L.: 2010, Rock burst process of limestone and its acoustic emission characteristics under true-triaxial unloading conditions. International Journal of Rock Mechanics and Mining Sciences, 47, No. 2, 286–298. DOI: 10.1016/j.ijrmms.2009.09.003

Holub, R.F. and Brady, B.T.: 1981, The effect of stress on radon emanation from rock. Journal of Geophysical Research, 86, No. B3, 1776–1784. DOI: 10.1029/JB086iB03p01776

Hutter, A.R.: 1996, Spatial and temporal variations of soil gas ^{220}Rn and ^{222}Rn at two sites in New Jersey. Environment International, 22, No. S1, 455–469. DOI: 10.1016/S0160-4120(96)00146-8

Jalili-Majareshin, A., Behtash, A. and Rezaei-Ochbelagh, D.: 2012, Radon concentration in hot springs of the touristic city of Sarein and methods to reduce radon in water. Radiation Physics and Chemistry, 81, No. 7, 749–757. DOI: 10.1016/j.radphyschem.2012.03.015

King, C.Y. and Luo, G. 1990, Variations of electric resistance and H_2 and Rn emissions of concrete blocks under increasing uniaxial compression. Pure and Applied Geophysics, 134, No. 1, 45–56. DOI: 10.1007/BF00878079

Koike, K., Yoshinaga, T., Suetsugu, K., Kashiwaya, K. and Asaue, H.: 2015, Controls on radon emission from granite as evidenced by compression testing to failure. Geophysical Journal International, 203, No. 1, 428–436. DOI: 10.1093/gji/ggv290

Lamonaca, F., Nastro, V., Nastro, A. and Grimaldi, D.: 2014, Monitoring of indoor radon pollution. Measurement, 47, No. 1, 506–508. DOI: 10.1016/j.measurement.2013.08.058

Le, R.C. and Wang, X.Q.: 2006, Calculation and measurement of migration coefficient of radon under laboratory conditions. Nuclear Science and Techniques, 17, No. 2, 92–96. DOI: 10.1016/S1001-8042(06)60019-5

Malmqvist, L., Isaksson, M. and Kristiansson, K.: 1989, Radon migration through soil and bedrock. Geoexploration, 26, No. 2, 135–144. DOI: 10.1016/0016-7142(89)90058-6

Mollo, S., Tuccimei, P., Heap, M. J., Vinciguerra, S., Soligo, M., Castelluccio, M., Scarlato, P. and Dingwell, D. B.: 2011, Increase in radon emission due to rock failure: An experimental study. Geophysical Research Letters, 38, No. 14, L14304. DOI: 10.1029/2011GL047962

Nazaroff, W.W.: 1992, Radon transport from soil to air. Reviews of Geophysics, 30, No. 2, 137–160. DOI: 10.1029/92RG00055

Nguyen, D.C., Edward, C. and Lukasz, P.: 2005, Factors controlling measurements of radon mass exhalation rate. Journal of Environmental Radioactivity, 82, No. 3, 363–369. DOI: 10.1016/j.jenvrad.2005.02.006

Nicolas, A., Girault, F., Schubnel, A., Pili, E., Passelegue, F., Fortin, J. and Deldicque, D.: 2014, Radon emanation from brittle fracturing in granites under upper crustal conditions. Geophysical Research Letters, 41, No. 15, 5436–5443. DOI: 10.1002/2014GL061095.

Perrier, F. and Girault, F.: 2013, Harmonic response of soil radon-222 flux and concentration induced by barometric oscillations. Geophysical Journal International, 195, No. 2, 945–971. DOI: 10.1093/gji/ggt280

Rama. and Moore, W.S.: 1984, Mechanism of transport of U-Th series radioisotopes from solids into ground water. Geochimica et Cosmochimica Acta, 48, No. 2, 395–399. DOI: 10.1016/0016-7037(84)90261-8

Roy, A.K., Saha, A., Singh, R.P. and Sinha, R.M.: 2000, Application of soil radon and trace element geochemistry for uranium exploration at Kuchanapalle, Guntur District, Andhra Pradesh. Journal of Geological Society of India, 56, No. 1, 89–96.

Sakoda, A., Ishimori, Y. and Yamaoka, K.: 2011, A comprehensive review of radon emanation measurements for mineral, rock, soil, mill tailing and fly ash. Applied Radiation and Isotopes, 69, No. 10, 1422–1435. DOI: 10.1016/j.apradiso.2011.06.009

Schubert, M., Paschke, A., Lieberman, E. and Burnett, W.C.: 2012, Air-water partitioning of ^{222}Rn and its dependence on water temperature and salinity. Environmental Science & Technology, 46, No. 7, 3905–3911. DOI: 10.1021/es204680n

Soonawala N.M. and Telford, W.M.: 1980, Movement of radon in overburden. Geophysics, 45, No. 8, 1297–1315. DOI: 10.1190/1.1441125

Sun, H.B. and Furbish, D.J.: 1995, Moisture content effect on radon emanation in porous media. Journal of Contaminant Hydrology, 18, No. 3, 239–255. DOI: 10.1016/0169-7722(95)00002-D

Triantis, D., Anastasiadis, C. and Stavrakas, I.: 2008, The correlation of electrical charge with strain on stressed rock samples. Natural Hazards and Earth System Sciences, 8, No. 6, 1243–1248. DOI: 10.5194/nhess-8-1243-2008

Tuccimei, P., Mollo, S., Vinciguerra, S., Castelluccio, M. and Soligo, M.: 2010, Radon and thoron emission from lithophysae-rich tuff under increasing deformation: An experimental study. Geophysical Research Letters, 37, No. 5, L05305. DOI: 10.1029/2009GL042134

Varhegyi, A., Hakl, J., Monnin, M., Morin, J.P. and Seidel, J.L.: 1992, Experimental study of radon transport in water as test for a transportation microbubble model. Journal of Applied Geophysics, 29, No. 1, 37–46. DOI: 10.1016/0926-9851(92)90011-9

Walia, V., Lin, S.J., Fu, C.C., Yang, T.F., Hong, W.L., Wen, K.L. and Chen, C.H.: 2010, Soil-gas monitoring: A tool for fault delineation studies along Hsinhua Fault (Tainan), Southern Taiwan. Applied Geochemistry, 25, No. 4, 602–607. DOI:10.1016/j.apgeochem.2010.01.017

Wattananikorn, K., Kanaree, M. and Wiboolsake, S.: 1998, Soil gas radon as an earthquake precursor: Some considerations on data improvement. Radiation Measurements, 29, No. 6, 593–598. DOI: 10.1016/S1350-4487(98)00079-1

Wilkening, M.H. and Watkins, D.E.: 1976, Air exchange and Radon-222 concentration in the Carlsbad Cavens. Health Physics, 31, No. 2, 139-143.

Winkler, R., Ruckerbauer, F. and Bunzl, K.: 2001, Radon concentration in soil gas: A comparison of the variability resulting from different methods, spatial heterogeneity and seasonal fluctuations. Science of the Total Environment, 272, No. 1-3, 273–282. DOI: 10.1016/S0048-9697(01)00704-5

Wysocka, M.: 2010, Radon in the investigations of geo-hazards in Polish collieries. Geofluids, 10, No. 4, 564–570. DOI: 10.1111/j.1468-8123.2010.00306.x

Xue, S., Dickson, B. and Wu, J.: 2008, Application of ^{222}Rn technique to locate subsurface coal heatings in Australian coal mines. International Journal of Coal Geology, 74, No. 2, 139–144. DOI: 10.1016/j.coal.2007.11.005

Xue, S., Wang, J., Xie, J. and Wu, J.: 2010, A laboratory study on the temperature dependence of the radon concentration in coal. International Journal of Coal Geology, 83, No. 1, 82–84. DOI: 10.1016/j.coal.2010.03.003

Zhang, W., Zhang, D.S., Ma, L.Q., Wang, X.F. and Fan, G.W.: 2011, Dynamic evolution characteristics of mining-induced fractures in overlying strata detected by radon. Nuclear Science and Techniques, 22, No. 6, 334–337. DOI: 10.13538/j.1001-8042/nst.22.334-337

Zhang, W., Zhang, D.S., Wang, X.F., Xu, M.T. and Wang, H.Z.: 2014, Analysis of mathematical model for migration law of radon in underground multilayer strata. Mathematical Problems in Engineering, 2014 (1), 250852. DOI: 10.1155/2014/250852

Zhang, W., Zhang, D.S., Wu, L.X. and Wang, H.Z.: 2014, On-site radon detection of mining-induced fractures from overlying strata to the surface: A case study of the Baoshan Coal Mine in China. Energies, 7, No. 12, 8483–8507. DOI: 10.3390/en7128483

Zhao, Y.J. and Wu, J.M.: 2003, Study on mechanism of detecting underground fire by radon measurement technique. Journal of China Coal Society, 28, No. 6, 260–263, (in Chinese). DOI: 10.13225/j.cnki.jccs.2003.03.008